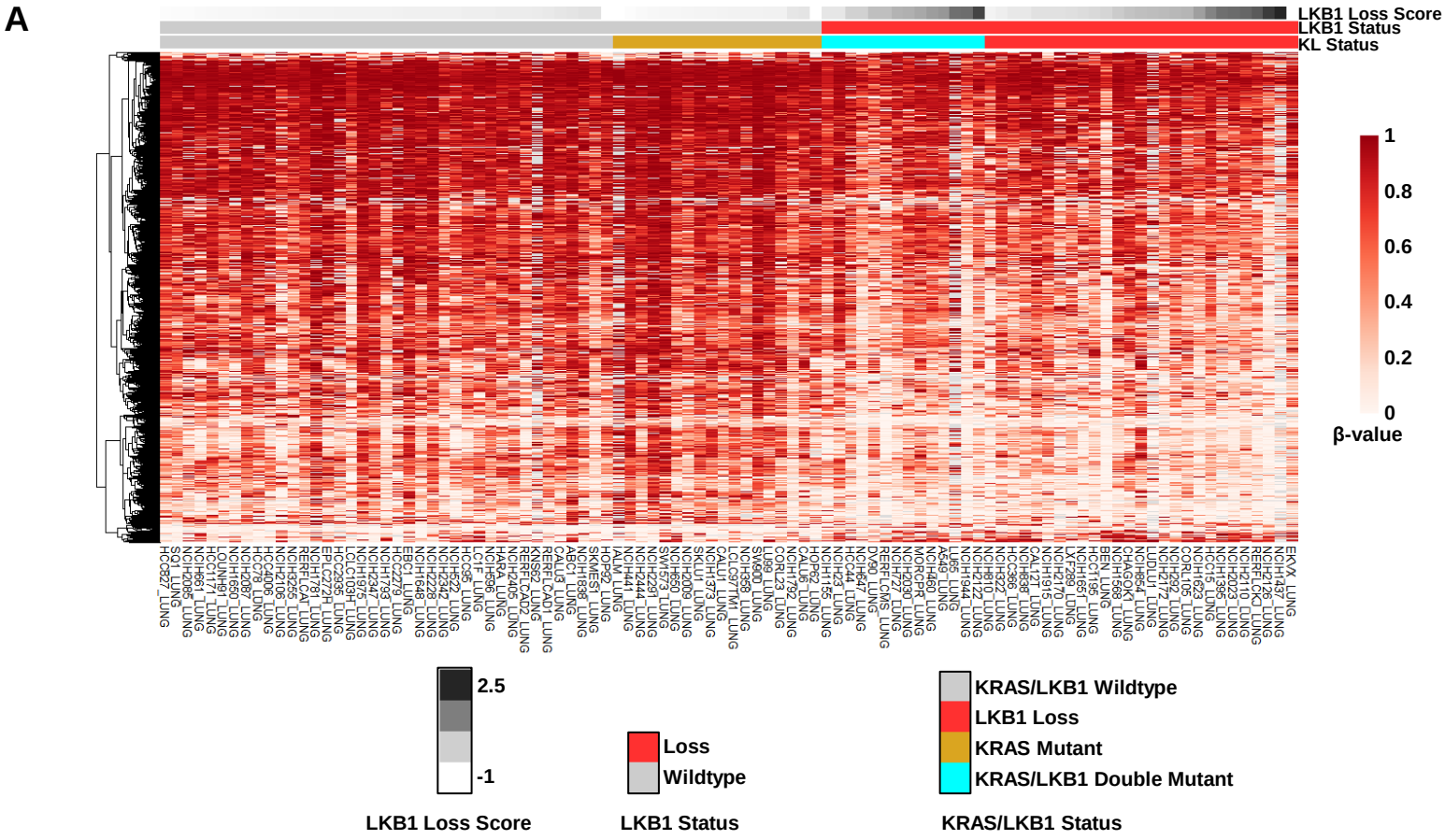

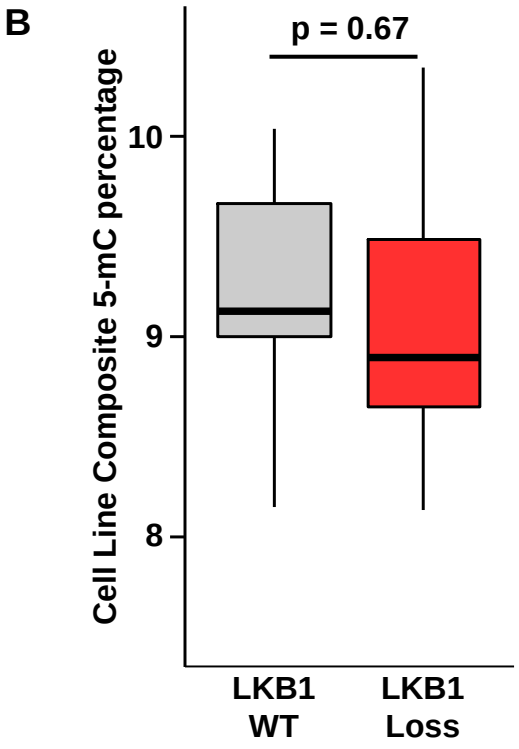

Supplemental figure 1: Comparison of CpG methylation and 5-mC concentration among NSCLC cell lines. (A) Clustering and heatmap visualization was performed on the top 5000 differentially methylated probes between LKB1-loss and LKB1-WT groups in the CCLE RRBS dataset. Samples were ranked by LKB1-loss signature score. (B) 5-mC concentration was measured in H358 and Calu-1 cells with LKB1 knockout and A549 cells with LKB1 addback using an ELISA-based approach. In a combined comparison among all cell lines tested there were no significant differences observed by Student 2-sample t-test.

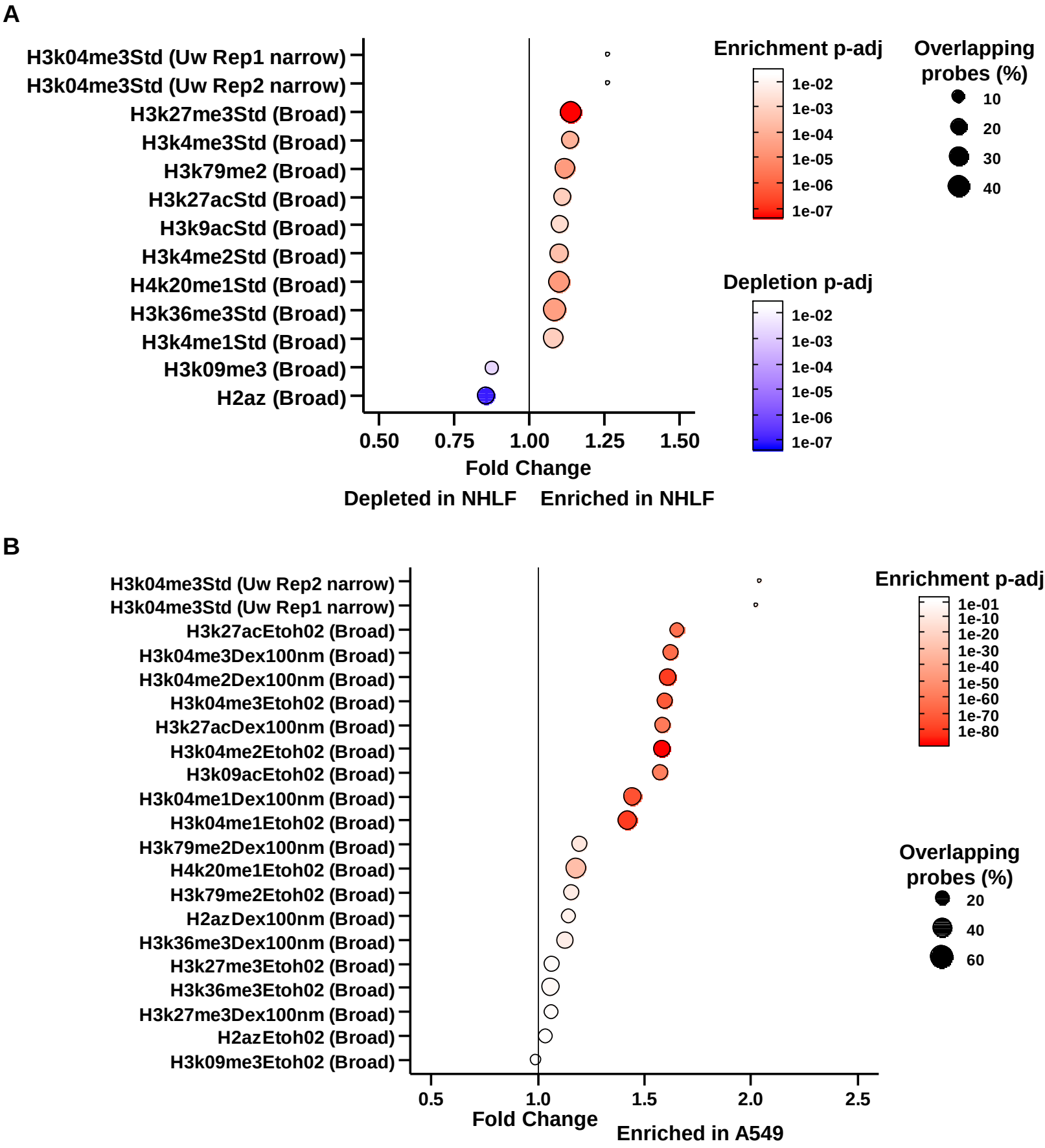

Supplemental figure 2: Enrichment of NHLF/A549 histone marks at sites hypomethylated in human lung cancer shows enrichment of active chromatin marks. (A) The top 5000 sites hypomethylated in LKB1-loss vs LKB1-WT lung adenocarcinoma were examined for histone mark enrichment at those sites in normal human lung fibroblasts (NHLF) in the ENCODE database. (B) The top 5000 probes hypomethylated in LKB1-loss vs LKB1-WT lung adenocarcinoma were examined for histone mark enrichment at those sites in lkb1-loss A549 cells in the ENCODE database.

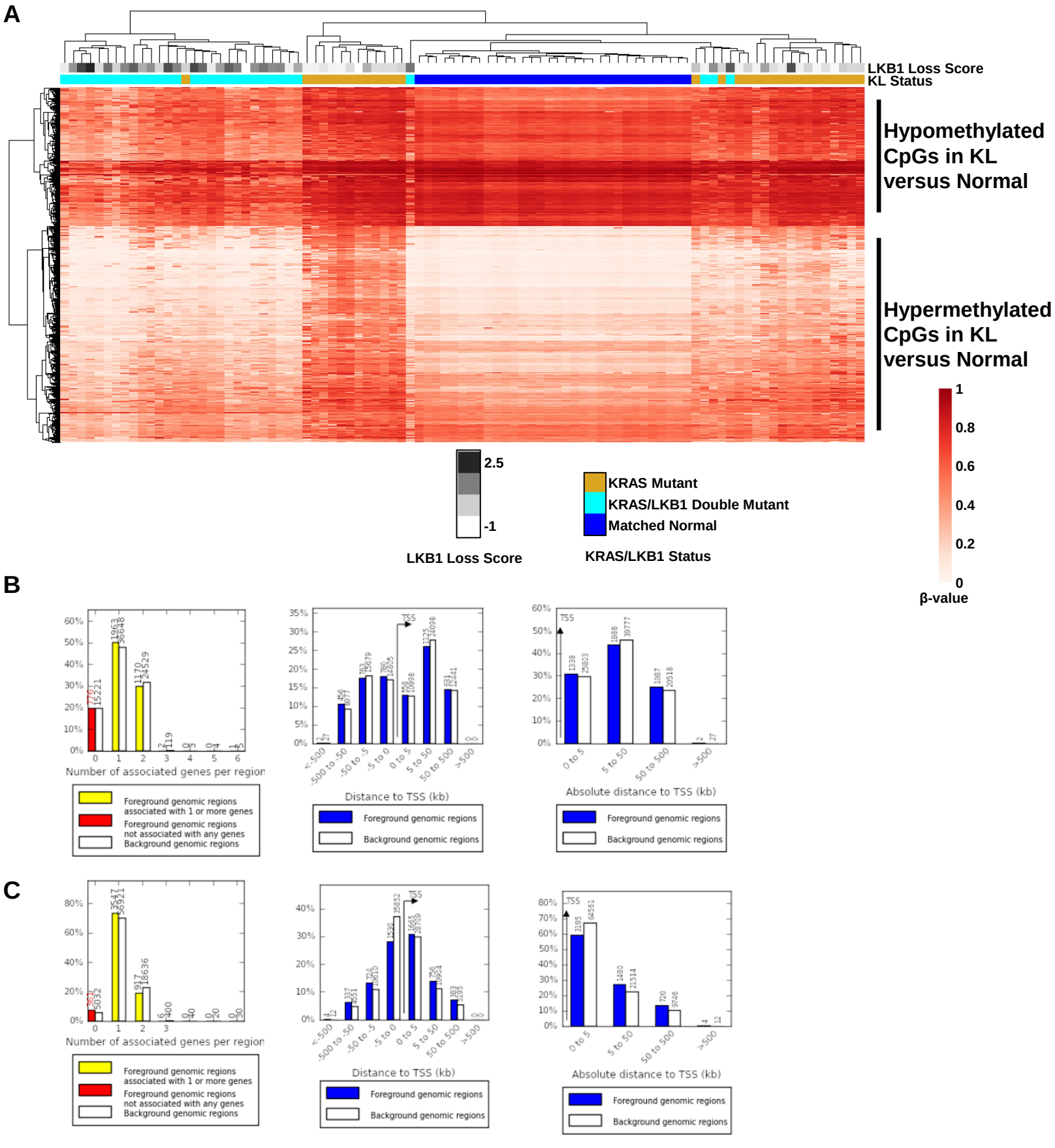

Supplemental figure 3: Comparison of LKB1/KRAS and KRAS mutant lung adenocarcinoma to matched normal. (A) (C) Clustering and heatmap visualization was performed on the top 5000 differentially methylated probes between KL and K tumors. Unsupervised clustering was used to compare the β-values at these differentially methylated loci. The results suggest that KRAS-mutant, LKB1-loss (KL) lung cancers display two specific methylation trends—hypomethylation of CpGs compared to normal tissue and hypomethylation of CpGs compared to KRAS mutant tumors. (B) For hypomethylated CpGs in KL versus normal, the number of associated genes, relative distance to transcription start site, and absolute distance to transcription start site were compared to background probes (C) For hypermethylated CpGs in KL versus normal, the number of associated genes, relative distance to transcription start site, and absolute distance to transcription start site were compared to background probes.

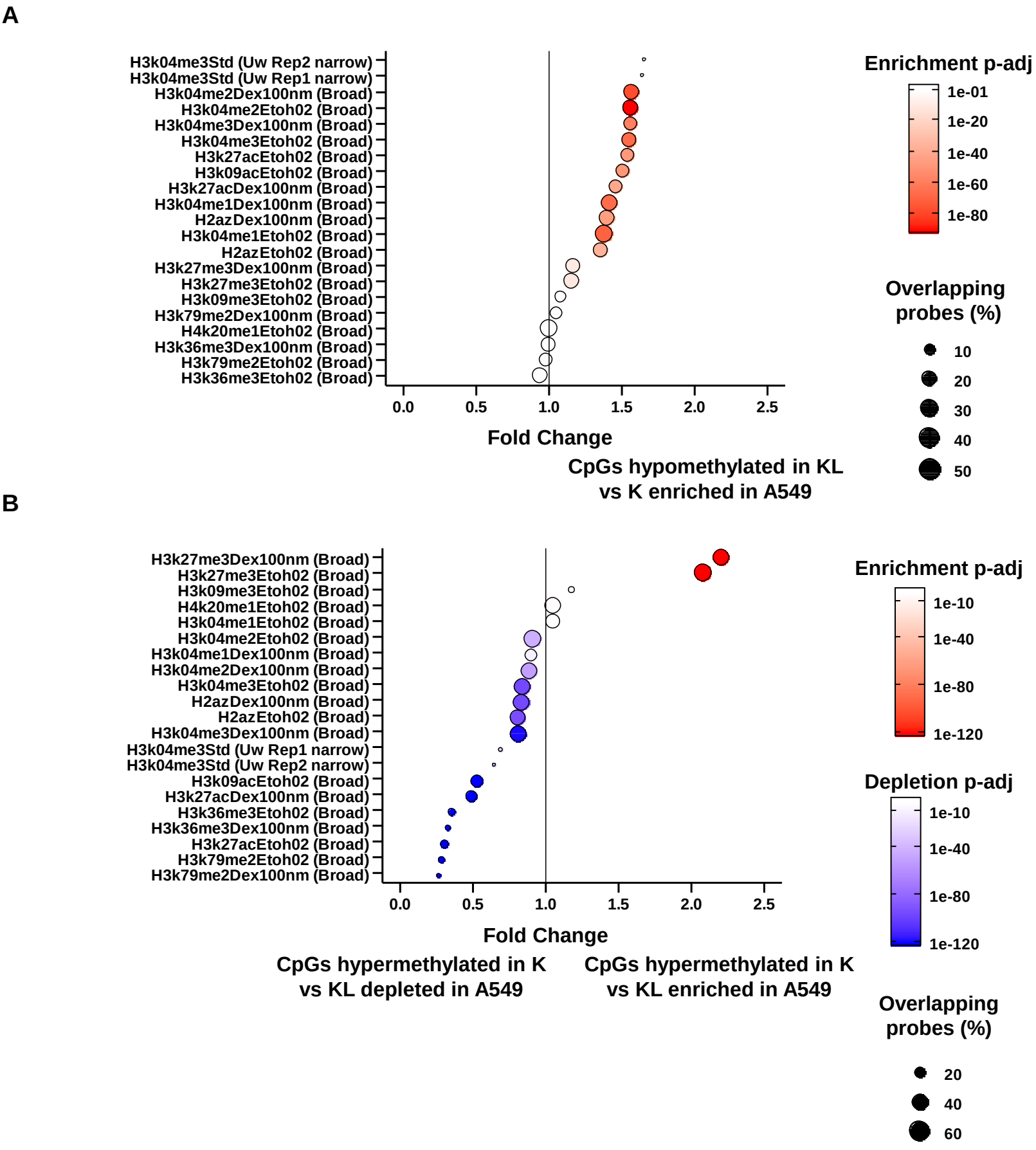

Supplemental figure 4: Enrichment of KL-specific hypomethylation sites and K-specific hypermethylated sites shows attenuation of polycomb repression in KL tumors. (A) the top 5000 KL-specific hypomethylated CpGs were compared to histone marks in A549 cells showing enrichment of H3K4me3, H3K27ac, and H3K9ac marks. (B) The top 5000 K-specific, CIMP-associated hypermethylated CpGs were compared to A549 histone marks and showed enrichment of H3K27me3 marks, which is a signature of polycomb repression.

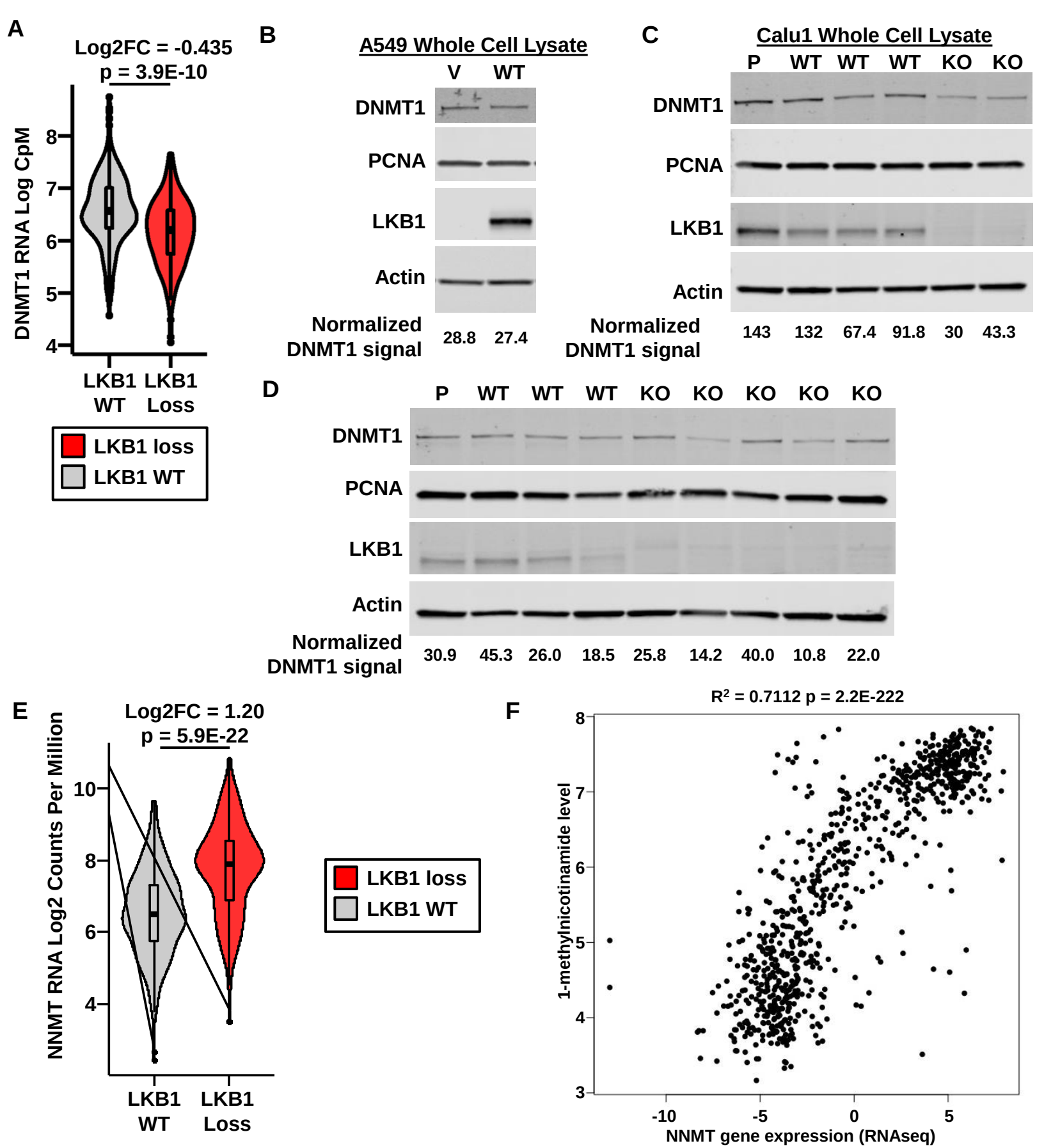

Supplemental figure 5: LKB1-loss tumors express significantly less DNMT1 and significantly more NNMT. (A) Expression of *DNMT1* RNA was significantly decreased in LKB1-loss TCGA samples. (B) untreated A549 cells (P) and A549 cells treated with pBABE-vector (V) or pBABE-LKB1 (WT) were assessed for DNMT1 expression by Western blot. (C) Untreated Calu1 cells (P) and Calu1 clones treated with untargeted gRNA (WT) or LKB1 knockout (KO) were assessed for DNMT1 expression by Western blot. (D) Expression of *NNMT* is significantly higher in LKB1-loss TCGA samples. (E) Levels of 1-methylnicotinamide are positively correlated with expression of *NNMT* in CCLE cell lines. The correlation coefficient is 0.843, the R^2 is 0.7112. Linear regression yielded a p-value of 2.2E-222.

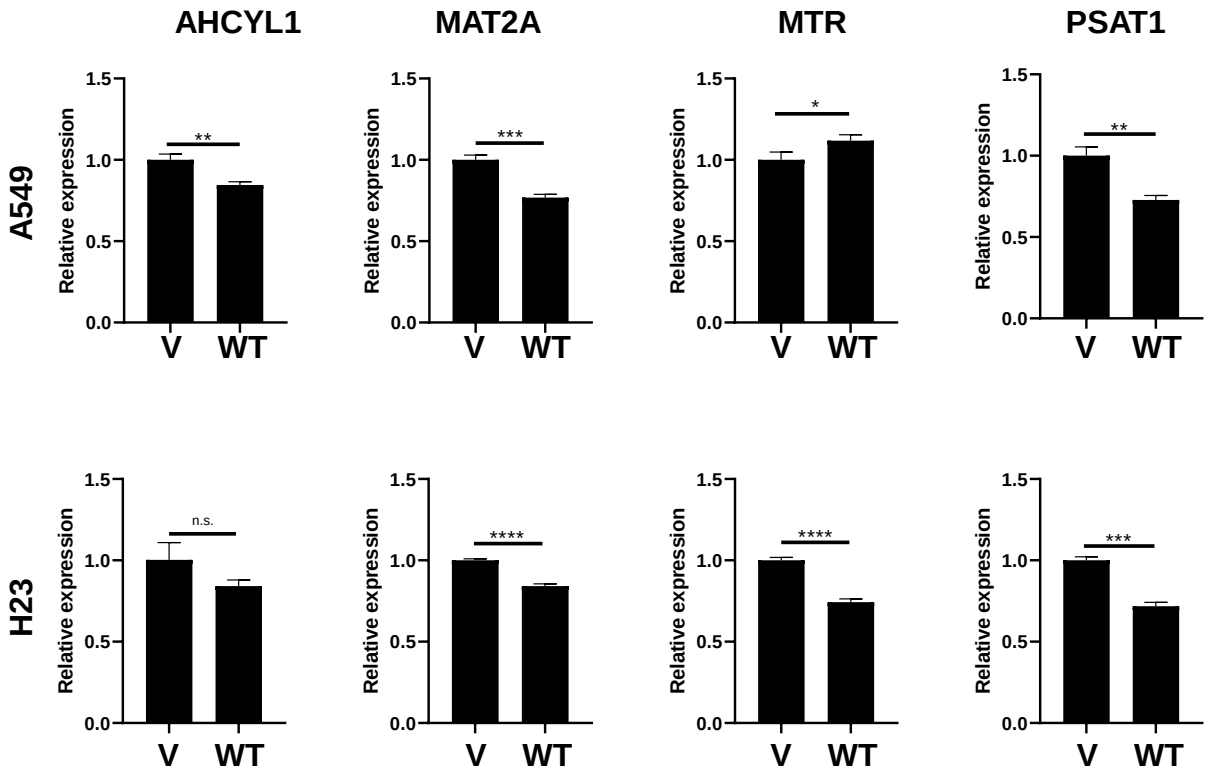

Supplemental figure 6: Expression of methionine cycle genes is significantly decreased with LKB1 overexpression in A549 and H23 cells. rtPCR of H23 and A549 cells following treatment with pBABE-vector (V) or pBABE-LKB1 (WT)shows a statistically significant decrease of *AHCYL1, MAT2A,* and *PSAT1* in both cell lines. MTR was only decreased in H23 cells.
(* p≤0.05, ** p≤0.01, *** p≤0.001, ****p≤0.0001).

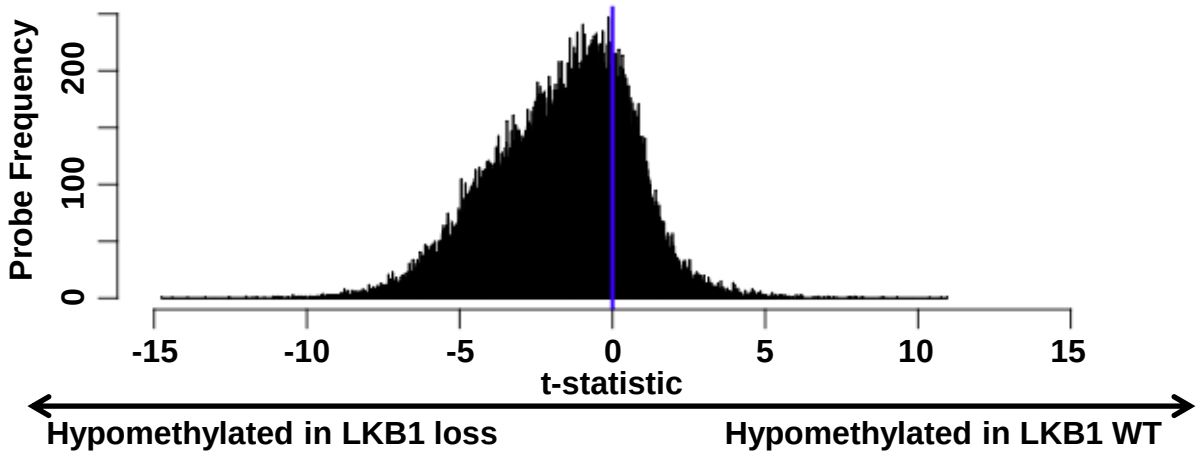

Supplemental figure 7: Repetitive elements are frequently hypomethylated in LKB1 loss lung adenocarcinoma. Illumina 450K probe IDs from TCGA that were also annotated as repetitive elements in the RepeatMasker database were selected and methylation β-values were compared between LKB1 loss and LKB1 WT tumors; t-statistics show a trend towards hypomethylation in repetitive elements.

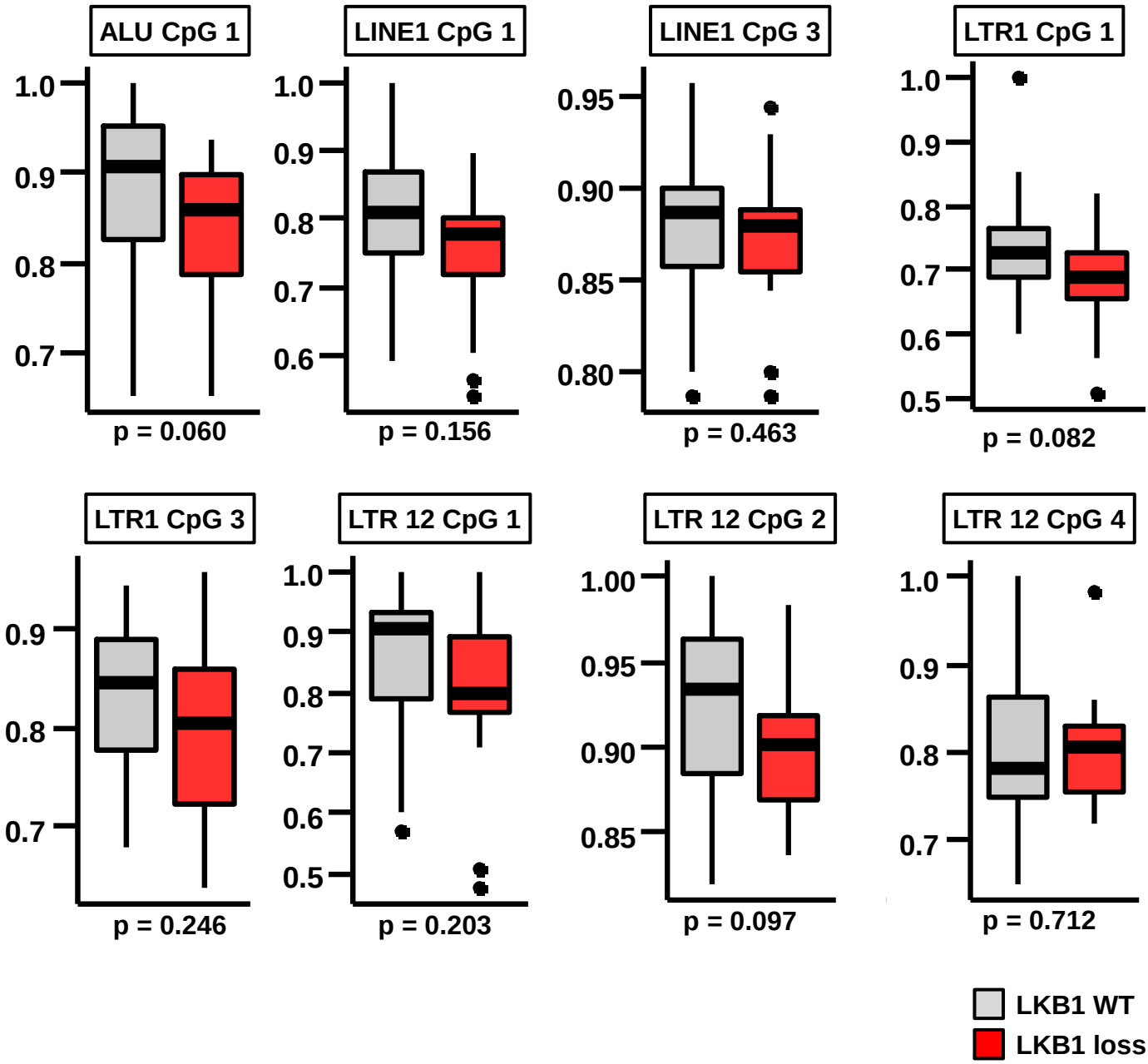

Supplemental figure 8: Repetitive element CpG demethylation in LKB1-loss human samples. Repetitive Element methylation in 54 resected lung adenocarcinomas was assessed using Epityper followed by MassARRAY. Comparisons were made by Wilcoxon signed-rank test with p-value adjustment using the Benjamini-Hochberg method.

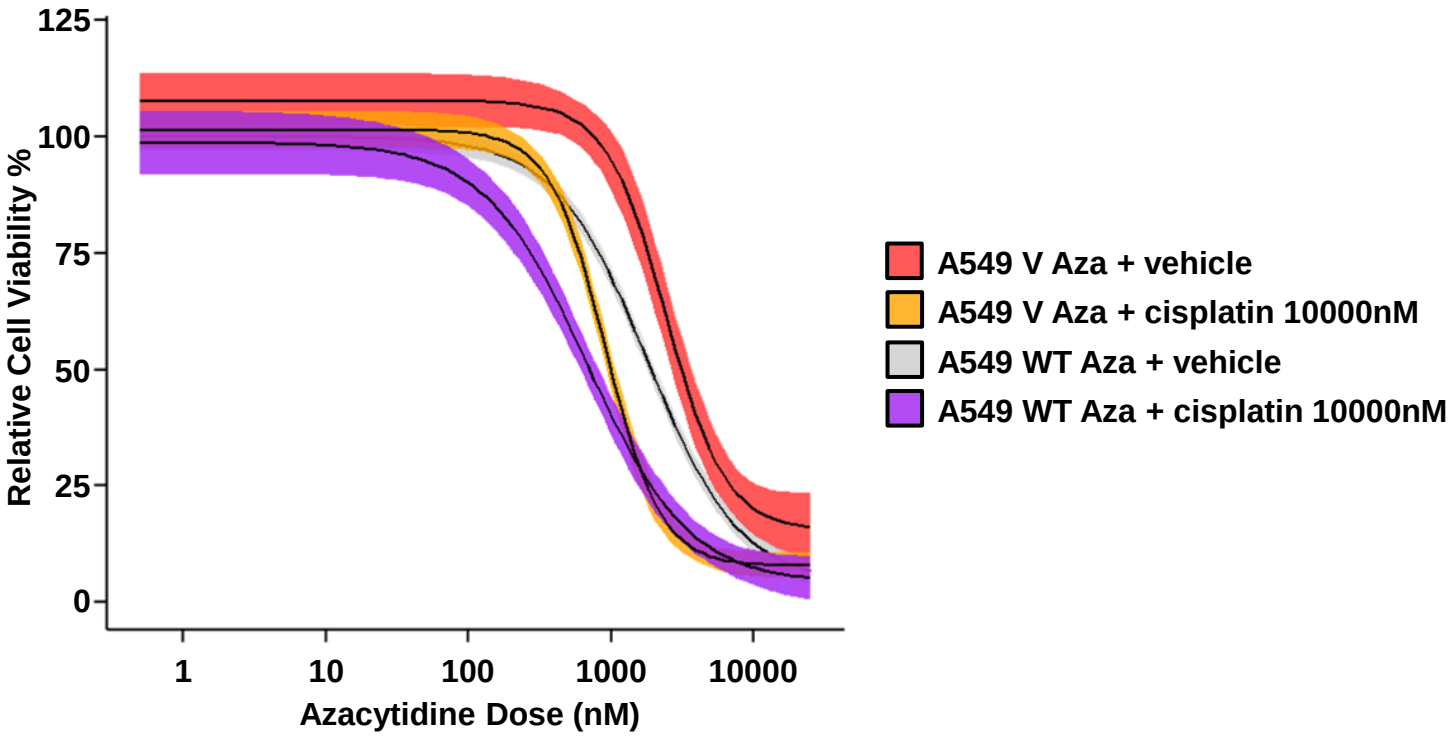

Supplemental figure 9: A549 cells treated with pBABE-vector (V) or pBABE-LKB1 (WT) were treated with azacytidine for 7 days, followed by cisplatin for 48 hours; viability data at the end of the experiment was fitted to a log-logistic model using the *drc* package in R.

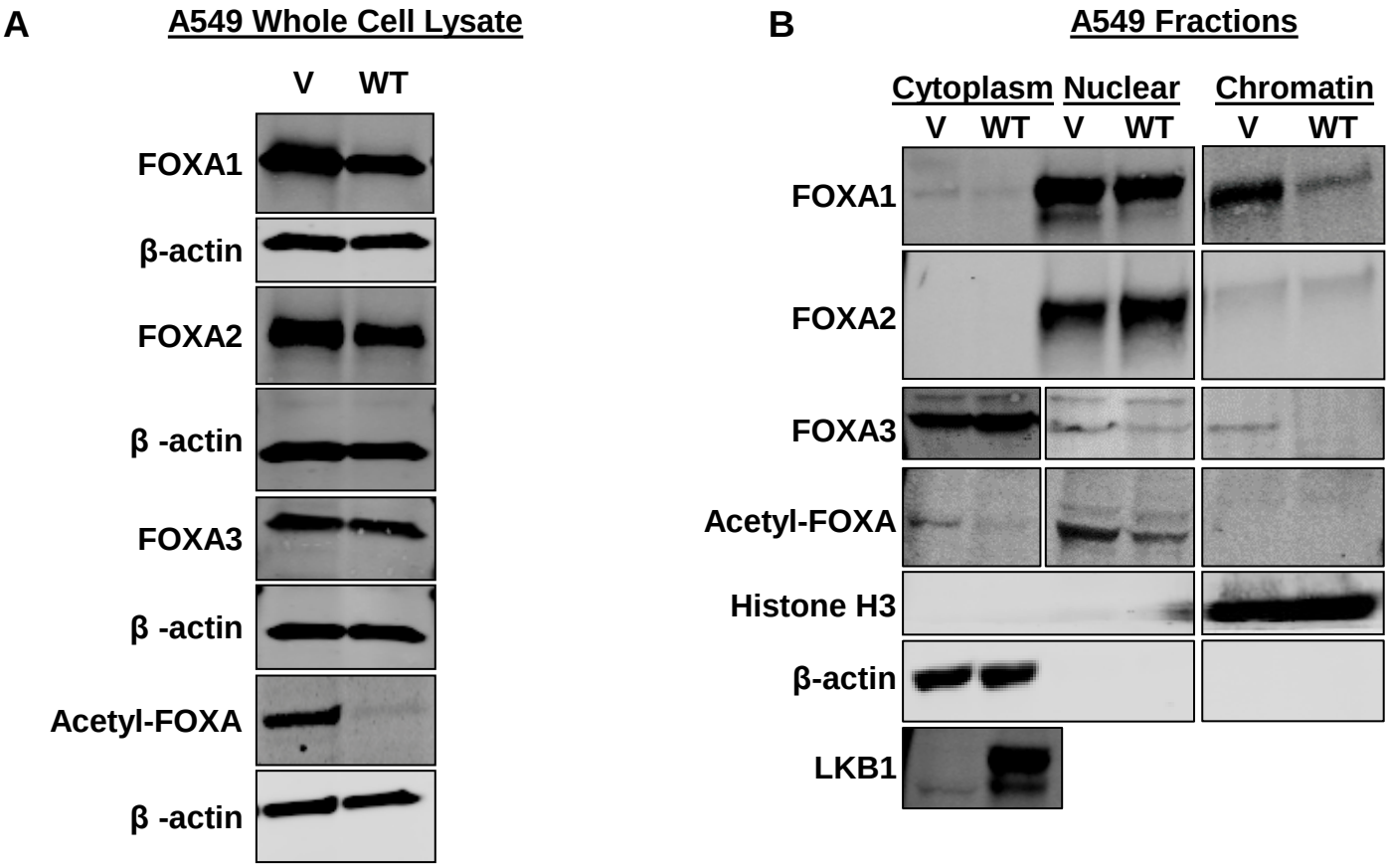

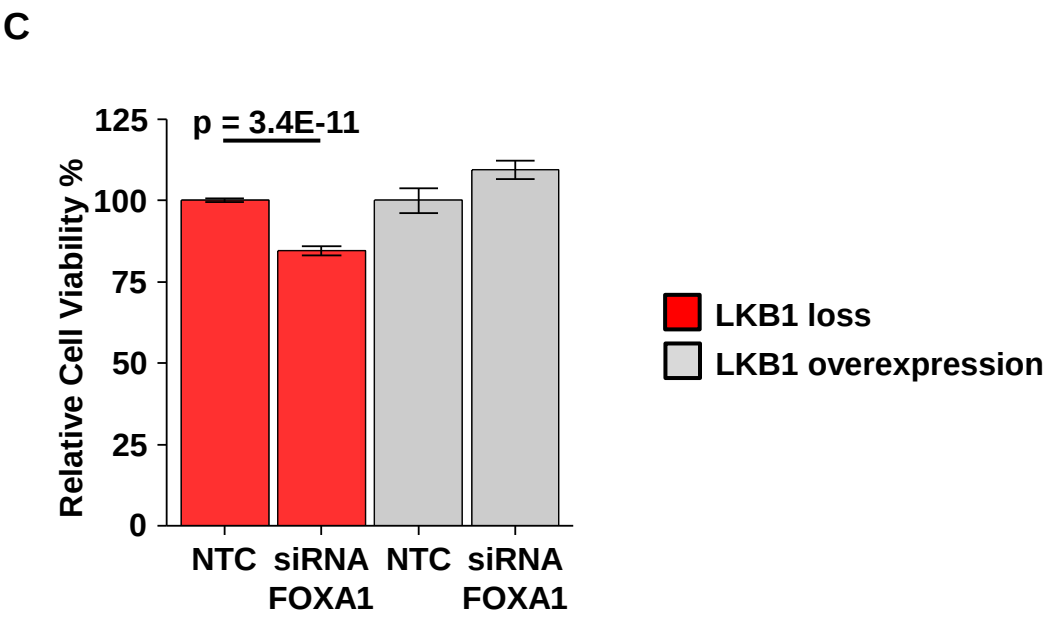

Supplemental figure 10: FOXA1 expression and chromatin binding of FOXA1 and FOXA3 is LKB1-dependent. LKB1-deficient A549 cells treated with pBABE-vector (V) or pBABE-LKB1 (WT) were assessed for FOXA1/2/3 and Acetyl-FOXA1/2/3 Lys264/253/211 via Western blot in both whole cell lysates (A) and fractionated lysates (B). Total expression of FOXA1, FOXA2 and Acetyl-FOXA is reduced following LKB1 addback; FOXA1 and FOXA3 chromatin binding is attenuated following LKB1 addback as well. Acetyl-FOXA is primarily located in the cytoskeletal compartment and is not seen in cytoplasmic or nuclear fractions. (C) A549 cells treated with pBABE-vector (V) or pBABE-LKB1 (WT) were subsequently treated with *FOXA1* siRNA treatment and viability was assessed using alamar blue assay.

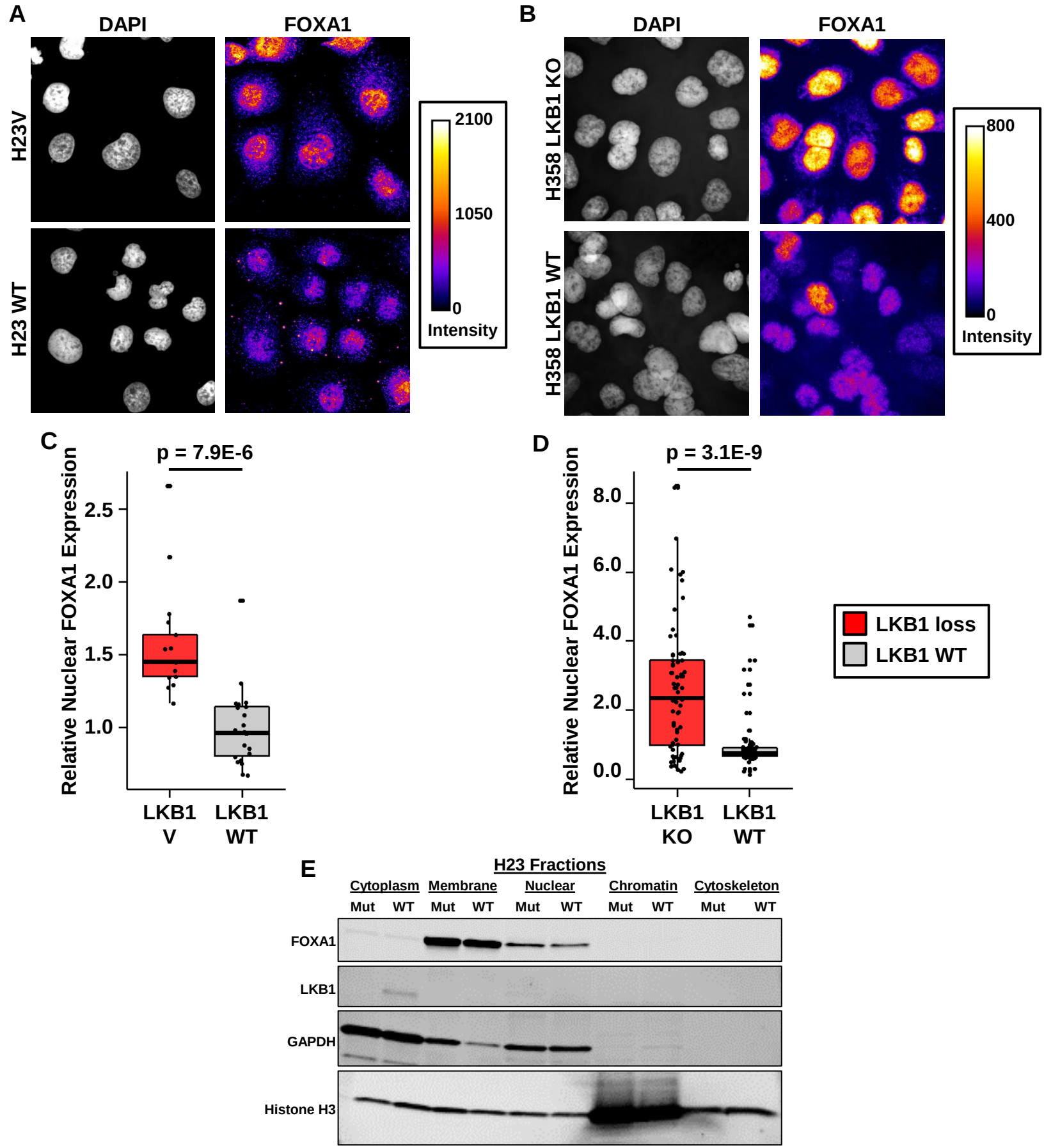

Supplemental figure 11: (A) Representative micrographs of FOXA1 nuclear localization and expression in H23 cells treated with pBABE-vector (V) or pBABE-LKB1 (WT). (B) Representative micrographs of FOXA1 nuclear localization and expression in H358 cells following LKB1 CRISPR knockout (KO) and in control wildtype (WT) clones. (C) Relative nuclear pixel intensity was calculated for H23 cells treated with pBABE-vector (V) or pBABE-LKB1 (WT) and compared using Student's t-test. (D) Relative nuclear pixel intensity was calculated for H358 cells following LKB1 CRISPR knockout (KO) and in control wildtype (WT) clones and compared using Student's t-test. (E) Western blot of FOXA1 nuclear localization and expression in H23 cells treated with pBABE-vector (V) or pBABE-LKB1 (WT).

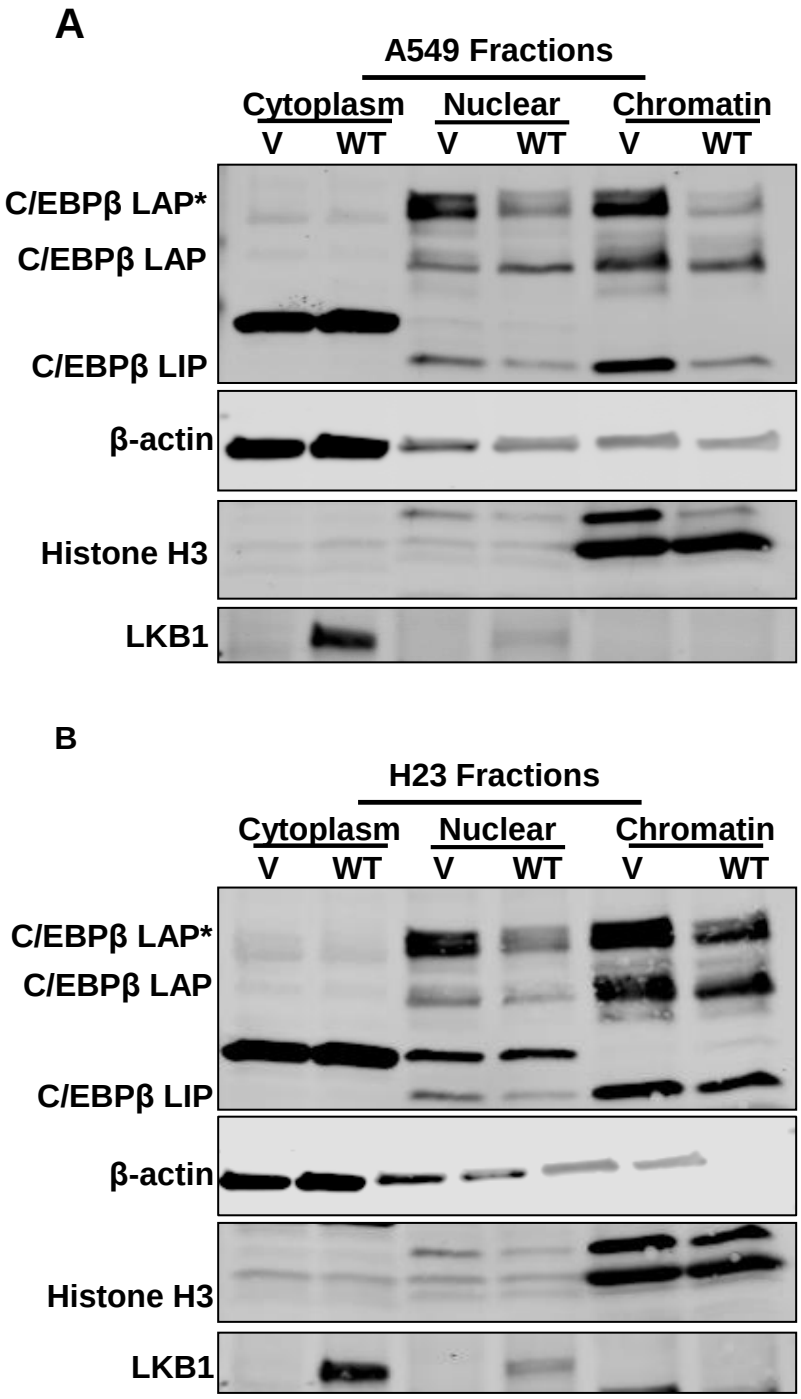

Supplemental figure 12: C/EBPβ localization in H23 and A549 cells is LKB1-dependent
LKB1-deficient (A) A549 and (B) H23 cells cells were treated with pBABE-vector (V) or pBABE-LKB1 (WT). . C/EBPβ localization subsequently analyzed via Western blot in fractionated lysates. Three C/EBPβ isoforms are identified: the Liver-enriched activator protein* (LAP*), the Liver-enriched activator protein (LAP), and the Liver-enriched inhibitory protein (LIP). Nuclear and chromatin-bound expression of C/EBPβ transcription-activating LAP isoforms is attenuated following LKB1 addback.

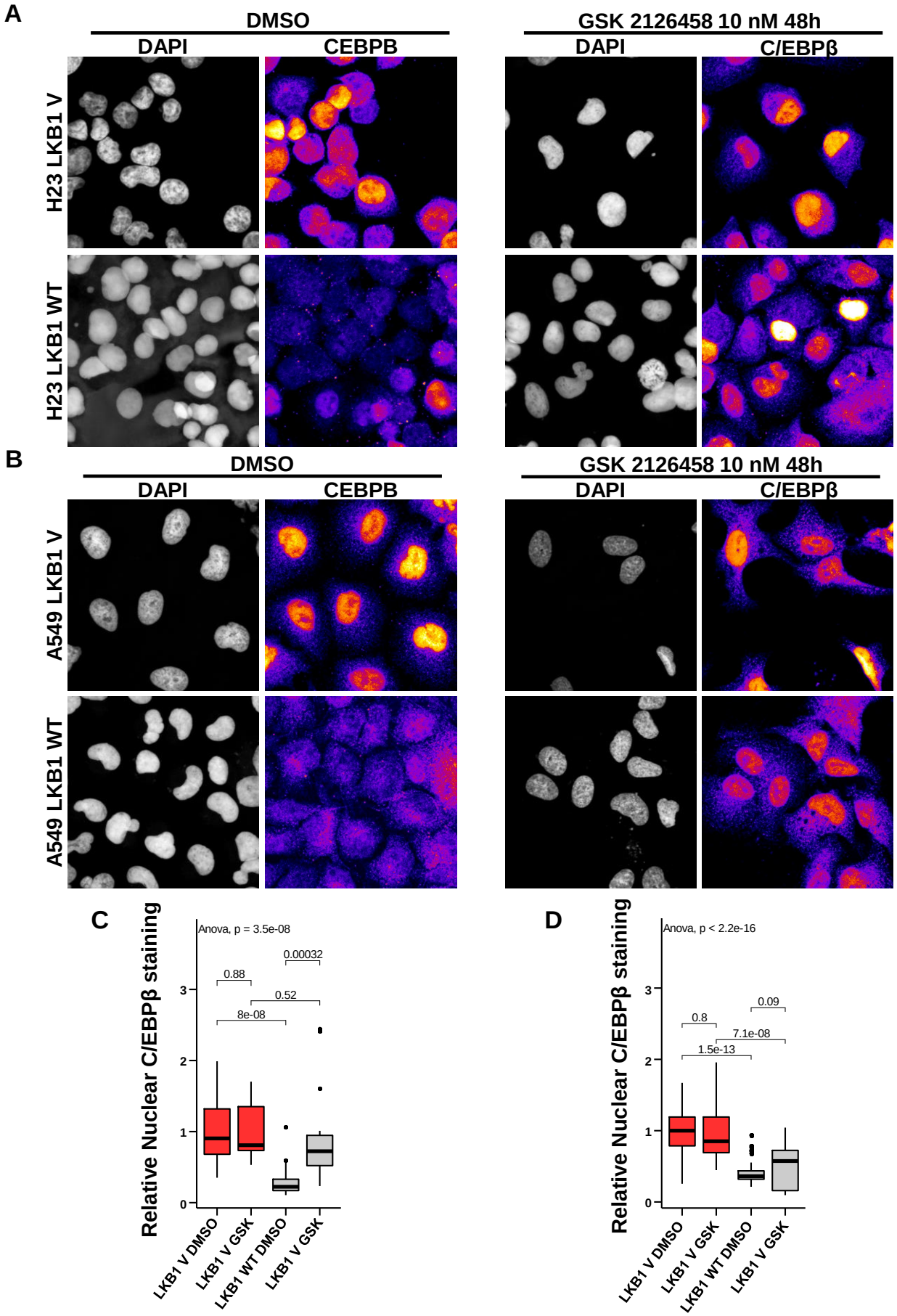

Supplemental figure 13: CCAT/Enhancer Binding Protein β (C/EBPβ) nuclear localization is dependent on LKB1 status and PI3K-mTOR function. (A) Representative micrographs of C/EBPβ nuclear localization and expression in H23 cells treated with pBABE-vector (V) or pBABE-LKB1 (WT) and DMSO vehicle versus GSK 2126458. (B) Representative micrographs of C/EBPβ nuclear localization and expression in A549 cells treated with pBABE-vector (V) or pBABE-LKB1 (WT) and DMSO vehicle versus GSK 2126458. (C) Relative nuclear pixel intensity was calculated for H23 cells treated with pBABE-vector (V) or pBABE-LKB1 (WT) and DMSO vehicle versus GSK 2126458 and compared using pairwise t-tests and ANOVA. (D) Relative nuclear pixel intensity was calculated for A549 cells treated with pBABE-vector (V) or pBABE-LKB1 (WT) and DMSO vehicle versus GSK 2126458 and compared using pairwise t-tests and ANOVA.